Co-propagating BoseEinstein condensates and electromagnetic radiation: formation of mutually localized structures

F Cattani, A Kim, D Anderson, M Lisak

Co–propagating Bose–Einstein Condensates and electromagnetic radiation: Formation of mutually localized structures

F Cattani[1], A Kim[2], D Anderson[3] and M Lisak[3]

[1] Department of Physics, Clarendon Laboratory, OX1 3PU, Oxford, UK
[2] Institute of Applied Physics, Russian Academy of Sciences, 603950 Nizhny Novgorod, Russia
[3] Department of Radio and Space Science, Chalmers University of Technology, SE-412 96 Göteborg, Sweden

E-mail: f.cattani1@physics.ox.ac.uk

Abstract.

A semi–classical model is derived for describing the interaction between coherent electromagnetic radiation and a Bose–Einstein condensate in the limit of zero temperature, including the back action of the atoms on the radiation. This model is used to analyze the problem of the self–consistent evolution of a laser beam and a BEC atomic beam. The mutual propagation is studied numerically and demonstrates the possibility of a stationary regime of mutual guiding, but also of generating a collapse–like phenomenon.

PACS numbers: 03.75.-b, 34.20.Cf, 34.80.Qb

Submitted to: *J. Phys. B: At. Mol. Opt. Phys.*

1. Introduction

The interactions between electromagnetic radiation and neutral atoms, and in particular their nonlinear aspects, have found an intriguing protagonist with the realization of coherent atomic beams, strong Bosonic degeneracy being the reason why Bose–Einstein condensates (BEC) are playing a major role in this research field. When considering coherent atomic beams, the intrinsic nonlinearity related to atom–atom interactions should be taken into account and, under the appropriate conditions, it can be described with a mathematical model strictly resembling that of the optical Kerr nonlinearity [1]. However, the presence of a light wave introduces more nonlinear features in the atom physics and we are interested in studying these effects from the point of view of atom manipulation and creation of localized light–atom structures.
The light wave acting as a nonlinear medium can mediate atomic interactions, in complete analogy to the role played by a nonlinear medium in the case of light nonlinearities. In the simplest model under dipole approximation, the electromagnetic radiation induces emission of dipole radiation which in turn gives rise to a long range interaction among the atoms, [2, 3]. This model has attracted much interest since the pioneering work of Askar'jan [4] and Ashkin [5] who demonstrated how it was possible to describe and test the effects of electromagnetic radiation on neutral atoms, which made it possible to focus atoms with light. Klimontovich and Luzgin then proceeded in showing how neutral atoms can focus light as a result of light pressure dipole forces, [6]. The main conceptual difference between those original models and the description of coherent atomic beams is due to the presence of long range coherence as pointed out by Saffman, [7], who modelled the contribution of light–mediated dipole–dipole interactions in terms of a contact potential while other authors worked out a description from first principles purely within the framework of quantum mechanics, [8, 9]. Efforts have also been made to go beyond the mean field approximation keeping into account as much as possible of the physics, including for example the effects of the inhomogeneity of the system and describing the physical effects that could be expected, see for instance [10]. Here we will consider a mean field model and in what follows, taking into account also the effects of the system inhomogeneity, we will give a description of the same phenomenon based on the analogy between matter waves and classical waves. We will then consider the possible formation of mutually localized structures and the possibility of having a collapse–like phenomenon even in one dimension.

2. Semiclassical approach

A semi–classical approach for describing the laser–induced atom interactions in a BEC was presented in [11], where the difference between the local field (the microscopic field acting on an atom) and the macroscopic field (the field averaged over a volume containing many atoms) was taken into account. Semi–classical reasoning leads to an extension of

the Gross–Pitaevskii equation normally used to describe BECs through the definition of laser–induced forces (striction forces) which, written as gradient forces, yield a potential energy in agreement with fully quantum mechanical results. To calculate these forces, Helmholtz considered the work done by the electric field on a dielectric, [12]. By working out the stress tensor through the variation of the dielectric free energy, an expression for the force was found for the case of a time independent electric field, [13]. This result was then generalized to the case of time dependent fields by Pitaevskii, [14], who showed that the expression for the stress tensor in this case is given by the time average of the same tensor calculated for a constant field. A straightforward application of Pitaevskii's results gives for the atom–atom interaction force induced by a far-off resonant laser field $\mathrm{Re}[\mathcal{E}\exp(-i\omega_L t)]$ on a zero-temperature, dilute BEC:

$$\mathbf{f} = \frac{n}{16\pi}\nabla\left[|\mathcal{E}|^2\frac{\partial\epsilon}{\partial n}\right], \tag{1}$$

where n is the condensate atom density and ϵ is the dielectric permittivity of the condensate gas which has to be suitably modelled. Quantum theory and macroscopic electrodynamics, [15], both yield

$$\epsilon = 1 + \frac{4\pi\alpha n}{1-\frac{4\pi}{3}\alpha n}, \tag{2}$$

where, as derived from quantum theory, $\alpha = -d^2/\hbar\Delta$ is the atomic polarizability at the laser frequency, with $\Delta = \omega_L - \omega_a$ being the detuning from the nearest atomic resonance frequency ω_a, and d is the dipole matrix element of the resonant transition. It is important to underline that (1) and (2) delimit the atomic physics we shall describe: The concept of force being a classical one, we will neglect quantum fluctuations, stochastic heating, incoherently scattered light and focus our attention on the coherent behaviour of the system. This limits the validity of the model mainly to large detunings $|\Delta| \gg \omega_a, \Gamma$ (where Γ is the atoms natural line width). Besides, any singularity occuring within this model is un–physical since losses and saturation effects (which are not accounted for) would then become important. Neglecting these effects allows us to study possible mutual localization mechanisms and, in the eventuality of collapsing cases, this analysis will be relevant for the evolution stage occurring before saturation mechanisms become important. The character of long range coherence is captured through the dipole–dipole interaction term.

The total force acting on a single atom is $\mathbf{F} = \mathbf{f}/n = -\nabla V_d$ and the generalized Gross–Pitaevskii equation for the condensate wave function $\Psi(\mathbf{r}, t)$ in the spirit of mean field theory reads, [1]:

$$i\hbar\frac{\partial\Psi}{\partial t} = \hat{H}_0\Psi + \left[U_0|\Psi|^2 - \frac{\alpha}{4}\frac{|\mathcal{E}|^2}{\left(1-\frac{4\pi}{3}\alpha|\Psi|^2\right)^2}\right]\Psi. \tag{3}$$

Here $\hat{H}_0$ is the linear single-particle Schrödinger Hamiltonian, the wave function Ψ is normalized as $N = \int|\Psi|^2 d\mathbf{r}$ with N denoting the total number of atoms, so that the gas density is $n = |\Psi|^2$, $U_0 = 4\pi\hbar^2 a_s/m$, m is the atom mass and a_s is the s–wave scattering

length which can be either positive or negative (repulsive or attractive collisional interaction). It must be kept in mind that this equation is valid for moderate laser intensities and for atom densities high enough to allow for a semi-classical description including near dipole-dipole interactions.
As already mentioned, effects of the laser–induced dipole–dipole interactions have been considered for instance in [7] or [8], but with a simplified interaction term, justified by the relatively low atomic densities and large detunings considered, which allowed an expansion of the potential energy term for $|\Psi|^2\alpha \ll 1$. This is the most important difference between the present work and [7] since a low density expansion makes the dipole interaction term independent of the sign of the detuning. It is natural, however, to expect that the structural dynamics of the condensate will depend on the nature of the nonlinearity, i.e. the sign of the detuning, and in the present investigation we will consider the fully nonlinear term. Depending on the sign of the detuning, the atom non linearity can have either a saturation character ($\Delta > 0$, blue detuning, i.e. $\alpha < 0$) or a singularity character ($\Delta < 0$, red detuning, i.e. $\alpha > 0$). By studying the consequences of the full non linear term on the density structures of an atomic beam copropagating with a laser beam, we expect to find an extension of well known results on cold atom guiding, see for instance [16] and references therein.

3. Basic equations

A first analysis which considered the full atomic nonlinearity but only a simplified description of the laser dynamics, predicted the formation of self–localized atomic structures, [11]. However, the feedback of the atoms on the laser was not taken into account and this effect may be of importance. In order to describe this feed back effect, it is necessary to include also a description of the evolution of the electromagnetic radiation, coupled to that of the atoms in order to analyze the possibility of mutual guiding and formation of localized structures.
The starting point are Maxwell's equations for propagation in a medium. Since we are interested in a stationary solution, we shall have

$$\mathbf{E}(\mathbf{r},t) = \mathrm{Re}[\mathcal{E}(\mathbf{r})\exp(-i\omega_L t)] \tag{4}$$

$$\Psi(\mathbf{r},t) = \Phi(\mathbf{r})\exp(-i\omega_a t). \tag{5}$$

Under the assumption of $L_n \gg \lambda_L$ or $\nabla\epsilon\cdot\mathbf{E} \simeq 0$ where L_n is the characteristic length scale of transverse density modulations and λ_L is the radiation wavelength, we have from $\nabla\cdot\mathbf{D} = 0$ that $\nabla\cdot\mathbf{E} \simeq 0$ and the wave equation

$$\nabla\times\nabla\times\mathbf{E} + \frac{1}{c^2}\frac{\partial^2\mathbf{D}}{\partial t^2} = 0 \tag{6}$$

given (2), becomes ($\omega_L = k_L c$)

$$\nabla^2\mathcal{E} + k_L^2\left(1 + \frac{4\pi\alpha|\Phi|^2}{1-\frac{4\pi}{3}\alpha|\Phi|^2}\right)\mathcal{E} = 0 \tag{7}$$

which corresponds to three scalar equations for the three components of the electromagnetic field.
This equation is further simplified by using the slowly varying envelope approximation, i.e. writing

$$\mathcal{E}(\mathbf{r}) = a(\mathbf{r}_\perp, z)\exp(ik_L z)\mathbf{e}, \tag{8}$$

$$\Phi(\mathbf{r}) = \psi(\mathbf{r}_\perp, z)\exp(ik_a z), \tag{9}$$

where $\mathbf{r}_\perp$ denotes the dimensions transverse to the propagation direction z, $\mathbf{e}$ is the polarization vector of the field and k_a is the atom wave number. The coupled system of equations (3), (7), can then be written in normalized variables as

$$i\mu\frac{\partial\tilde{\psi}}{\partial\tilde{z}} = -\frac{1}{2}\tilde{\nabla}_\perp^2\tilde{\psi} + \frac{1}{2}\beta_{coll}|\tilde{\psi}|^2\tilde{\psi} - \frac{s}{2}\frac{|\tilde{a}|^2}{\left(1-s|\tilde{\psi}|^2\right)^2}\tilde{\psi} \tag{10}$$

$$i\frac{\partial\tilde{a}}{\partial\tilde{z}} = -\frac{1}{2}\tilde{\nabla}_\perp^2\tilde{a} - \frac{3s}{2}\frac{|\tilde{\psi}|^2\tilde{a}}{1-s|\tilde{\psi}|^2}, \tag{11}$$

where the following normalisation has been used: $\tilde{\mathbf{r}} = \mathbf{r}k_L$, for the atom wave function $\tilde{\psi} = \psi/\psi_*$ with $(4\pi|\alpha|/3)\psi_*^2 = 1$, for the laser $\tilde{a} = a/a_*$, with $m|\alpha|a_*^2/(2\hbar^2k_L^2) = 1$, $s = sign(\alpha)$, $\mu = k_a/k_L$ and $\beta_{coll} = 6a_s/(k_L^2|\alpha|)$. The tilde will be dropped hereafter unless otherwise stated.
If the assumption of a classical model for the laser field is justified by the choice of the intensity regime, it is clear that, for a mean field model to be valid based on the simplest possible approximation to the many–body atomic wave function, we must consider not only a zero temperature limit but also a low density limit with $na_s^3 \ll 1$, see [17]. It will be shown hereafter that the parameter range in which we are interested is such as to satisfy this requirement.
We note that, although the laser equation is formally linear, it will nevertheless involve non-linear evolution due to the presence of the $|\psi|^2$ term. For simplicity, in all studied cases we assume $\mu = 1$ and consider one transverse dimension only, $r_\perp = x$, assuming that the system has a very large extension in y and can be considered as homogeneous in that direction. It is possible to find exact localized, stationary solutions via the shooting method which will be discussed elsewhere, [18]. Our main concern in the present investigation is how the initial transverse distributions of atom density ($|\psi(x,0)|^2$) and laser intensity ($|a(x,0)|^2$) vary during propagation along z.

4. Laser and BEC atomic beam propagation

From the point of view of physical effects, the most interesting case is that of an initially flat laser intensity profile where no gradient forces due to the electromagnetic radiation are present at the beginning of the propagation. As already pointed out by Saffman, [7], spatial gradients can grow even on such an homogeneous intensity profile. However, in contrast with [7], we do not consider an explicit non linearity for the laser equation and

in our case such gradients will be due to the effect of the atoms only. To gain insight on the physics acting during the very first stage of propagation, it is useful to look at the evolution of the laser intensity profile.

4.1. Initial laser evolution

In general, we may describe the propagating laser pulse amplitude as proportional to $exp\,(ihx + ikz)$ where neither h nor k are known. The "group velocity" of the pulse along x during propagation is $v_x = -\partial k/\partial h|_{h_0}$ (where h_0 is the central wave number in x, which is assumed to be zero). We expect the laser profile to diffract along x during the pulse propagation along z and the role of the atoms must be clarified. With an initially flat amplitude profile (e.g., supergaussian) the second derivative with respect to x in (11) can be safely neglected. Thus the presence of the atoms translates into a chirp on the laser transverse wave number as can be seen by separating real and imaginary part in (11), discarding the second derivative and solving for the laser amplitude $|a|$ and phase φ ($a = |a|exp(i\varphi)$). Straightforward algebra gives $\varphi = 2\pi k_L \alpha |\psi|^2 z/(1 - 4\pi\alpha|\psi|^2/3)$. The effect of such a chirp is well known in optics and it can be understood by noting that the modified phase $\varphi(x, z)$ induces a modification in the propagation velocity along x of the different Fourier components of the pulse. In fact, we can now write for the propagating pulse $|a|exp\,(i\varphi(x) + ikz)$ which shows how the chirp effect is to create an instantaneous x–wave number, [20],

$$h_c = \frac{\partial\varphi}{\partial x} = \frac{2\pi\alpha k_L z}{\left(1 - \frac{4\pi}{3}\alpha|\psi|^2\right)^2}\frac{\partial|\psi|^2}{\partial x}. \tag{12}$$

i.e., $h = h_0 + h_c$. Assuming an initial Gaussian form for the atom wave function well localized within the laser intensity distribution, the qualitative behaviour of the chirp as a function of x is shown in figure.1. Since we have‡ $dv_x/dh = -\partial^2 k/\partial h^2|_{h_0} > 0$, parts of the pulse with $h > h_0$ whill have a higher propagation velocity along x and viceversa. Looking at figure1, we expect that those parts of the pulse that are localized around the positive peak of the chirp function will move with higher velocities in the direction of positive x while those parts of the pulse that are localized around the negative peak will slow down. In the red detuning case, this creates a central peak in the laser intensity profile and two symmetric troughs where the chirp effect is stronger and empties the pulse. This is clearly seen in the numerical simulations immediately after the simulations start. In the blue detuning case, the result of the chirp effect is the opposite, thus the seed for further evolution depends on the sign of the detuning. An example of the modification induced on the laser intensity profile can be seen in figure2 for two runs with the same initial conditions but opposite sign of the detuning. Once this initial change in the laser structure is formed, it drives a dynamical reaction on the

‡ As can be seen by Taylor–expanding $k = k(h_0) + \partial k/\partial h|_{h_0}(h - h_0) + 1/2\partial^2 k/\partial h^2|_{h_0}(h - h_0)^2 + \ldots$. According to the usual transformation $ik \leftrightarrow i\partial/\partial z$ from the expansion for k we obtain an equation for the laser amplitude which corresponds exactly to our (11) if $\partial^2 k/\partial h^2|_{h_0} < 0$

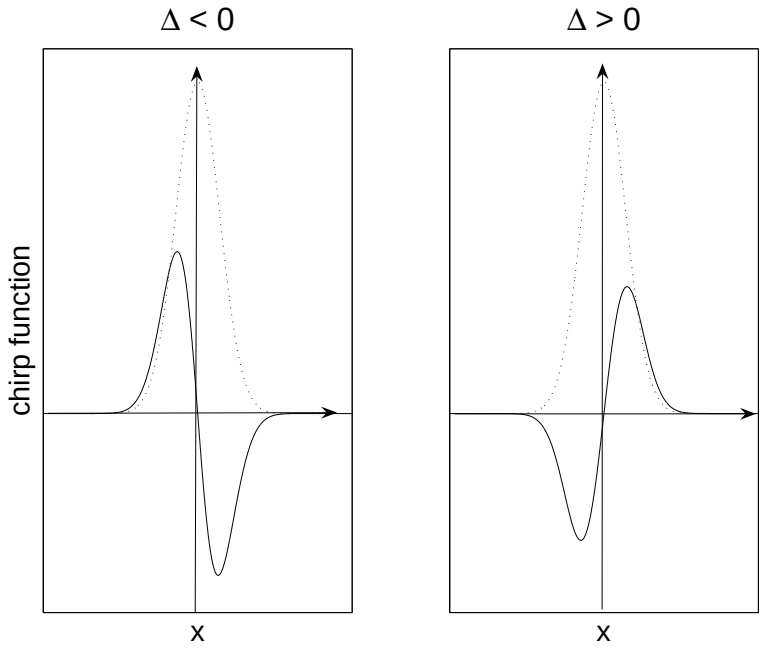

Figure 1. Qualitative behaviour of the chirp function (12), solid line, for an initial Gaussian atom density distribution, dashed line. Left: Red detuning, i.e. $sign(\alpha) > 0$; right: Blue detuning, i.e. $sign(\alpha) < 0$

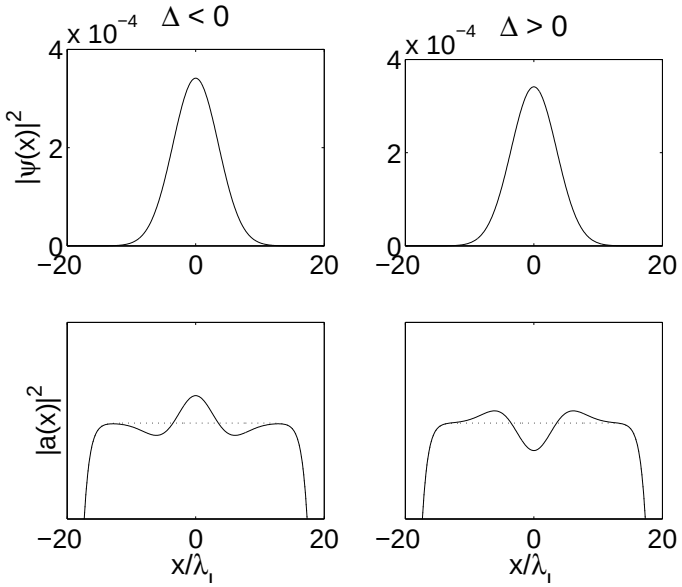

Figure 2. Atom density and laser intensity (detail of flat top) for red detuning (left) and blue detuning (right) after a very short propagation ($z = 0.0012\lambda_L$). Dotted line: Initial intensity distribution. Parameters are the same as for run a, see text. Normalization as given in the text.

atom density since the potential now felt by the atoms has been modified. Again, the response will be different according to the sign of the detuning.

4.2. Red detuning

This is an interesting case since the atoms will feel a focusing action from the dipole–induced potential. In particular, such an action will be strenghten by the initial formation of a central peak in the laser intensity and may lead to a catastrophic instability with subsequent collapse *even in the one dimensional case*. As noticed above, the atom equation has a singular nonlinearity and we may define a critical atom density as $\psi_*^2 = 3/(4\pi|\alpha|)$ in unnormalized variables (i.e., $\psi_*^2 = 1$ normalized variables), dependent on the detuning and on the dipole moment. However, the presence of the collisional nonlinearity cannot be neglected and should play an even more important role as soon as the atom density undergoes focusing. For a negative scattering lenght, the more the atoms are focused the stronger the focusing action and this is expected to strictly limit the stability of the system against collapse. Whereas a repulsive collisional non linearity, acting in the same direction as the diffractive kinetic energy contribution, should tend to balance the focusing effect of the laser induced non linearity. The possibility to reach this equilibrium (i.e., a structure consisting of two stationary localized coupled solutions) depends on the initial conditions and, to our knowledge, cannot be studied analytically. We have investigated numerically the parameter range for stability/collapse at fixed initial width of both the supergaussian laser intensity and the gaussian atom density profile given as

$$\psi(x,0) = \psi_0 e^{\left(-x^2/2d_a^2\right)} \tag{13}$$

$$a(x,0) = a_0 e^{-\left(x^2/2d_L^2\right)^g} \tag{14}$$

where g is the supergaussian parameter ($g = 10$ in the simulations).
In order to describe the numerical results it is useful to present a reference case whith parameters such that the system settles down rather smoothly onto a stationary, mutually localized structure for both atom density and laser intensity. A possible such case (the one referred to as run (a), has $d_a = 5\lambda_L$, $d_L = 40\lambda_L$, initial peak atom density $5.81\,10^{-18} m^{-3}$ (corresponding to $\tilde{\psi_0}^2 = 3.41\,10^{-4}$), inital peak laser intensity $0.0153\,mW/cm^2$ (corresponding to $\tilde{a_0}^2 = 0.0181$), with $\beta_{coll} = 38$ which corresponds for instance to a detuning of 100 times the decay rate for ^{87}Rb atoms. From these initial conditions, the system stabilizes onto the localized structures shown in figure3, with the evolution of the peak atom density and laser intensity showing characteristic relaxation oscillations during the approach to the final stationary state, see figure4. The atom transient dynamics is governed by an interplay between their kinetic energy and interatomic repulsive interactions together with the focusing laser-induced potential. The atoms initially see a potential trap induced by the presence of the laser combined to a central repulsive barrier due to their own repulsive interaction, see inset in figure3.

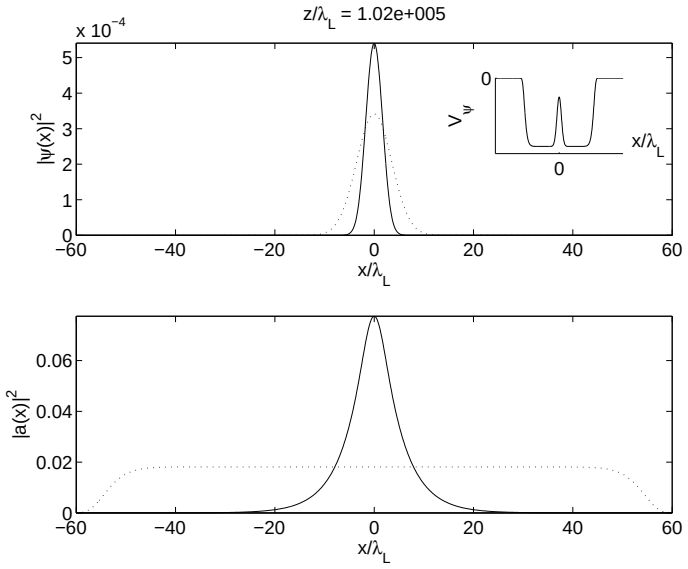

Figure 3. Stationary atom density and laser intensity after $1.02\ 10^5\lambda_L$ of propagation along z for run (a). Dotted lines: initial distributions. Normalization as in the text. The inset shows the potential initially felt by the atoms.

The natural thing to happen is for the atoms to escape from the central region where they are initially localized. The increase in the peak laser intensity (chirp effect) combined to the decrease in repulsion (decrease in the central atom density) both tend to create a central trap where initally there was a repulsive barrier, with the effect that some atoms remain centrally localized while those spreading out will move to encounter the lateral walls of the laser–induced potential trap.
The laser intensity profile tends to evolve according to what known for super–gaussian pulses (notice that initially $d_L >> d_a$), [21], forming modulations on its shoulders which in turn modify the laser–induced potential trap thus affecting the natural broadening of the atom wave function. Some atoms, and part of the electromagnetic radiation too, will escape out of the laser–induced trap but most of them in this case remain trapped and return back to interact with the central bunch. This process continues until a final stationary state is reached. Figure5 shows some snapshots of this evolution. The resulting structures have proved to be extremely robust against numerical perturbation tests.

Although, for fixed d_L/d_a, the physics of the laser evolution (i.e., central chirp, lateral modulation and shoulder formation) is qualitatively the same, the nature of the transient for the atoms changes depending on ψ_0/a_0 since the balance between the different effects changes as can be seen by looking at the initial potential felt by the atom wave function, see figure6.

Increasing the initial atom peak density, with fixed initial laser peak intensity, leads to the formation of mutually localized structures with higher and higher peak density, see figure 7(A). These results also give a good idea of what sort of physical parameters can be expected for these structures. For the initial conditions given in the caption of

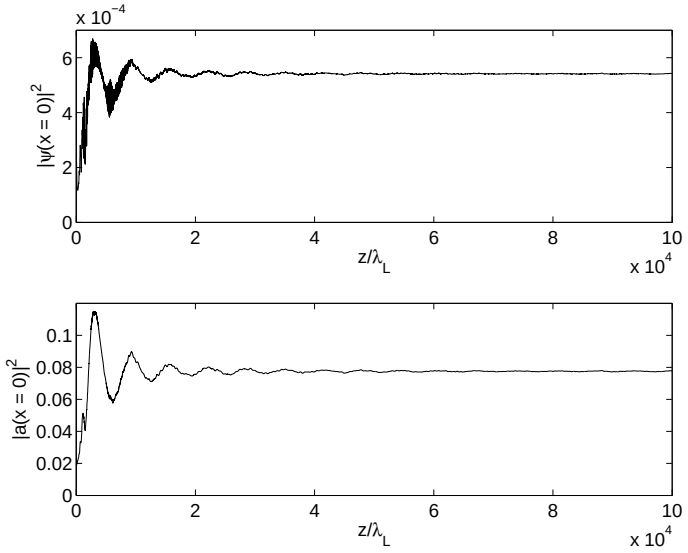

Figure 4. Peak atom density and laser intensity during propagation along z for run (a). Normalization as in the text.

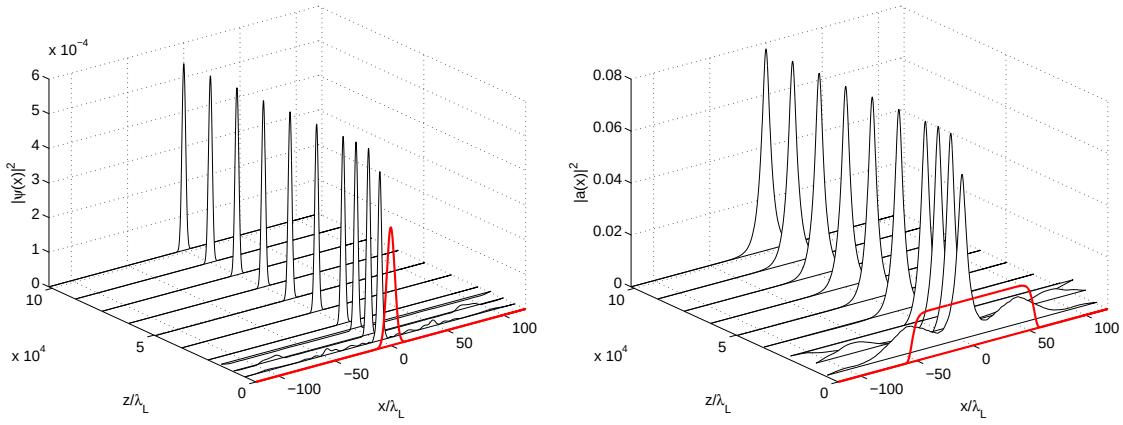

Figure 5. Snapshots of the evolution of atom and laser wave functions during propagation along z for run (a). In red the initial wave functions. Normalization as in the text.

figure 7(A) and an initial red detuning of about 3.81 GHz, i.e. 100 times the decay rate of ^{87}Rb of the $5^2S_{1/2} - 5^2P_{3/2}$ atomic resonance, the peak atom densities and peak laser intensities tend to settle down to values of the order of $10^{-19}\mathrm{m}^{-3}$ and $0.06\mathrm{mW/cm}^2$. The maximum peak atom densities and peak laser intensities reached during this evolution process are of the order of $1.8\,10^{19}\mathrm{m}^{-3}$ and $0.1\mathrm{mW/cm}^2$. Thus even at the maximum values reached, the low density condition $na^3 \ll 1$ still holds, being $na^3 \sim 10^{-5} - 10^{-6}$ for all cases of figure 7.

In the model we have presented, all absorption processes were neglected, a legitimate assumption provided that the laser detuning Δ is so large compared with the spontaneous emission rate that the imaginary part of the dielectric permittivity can be

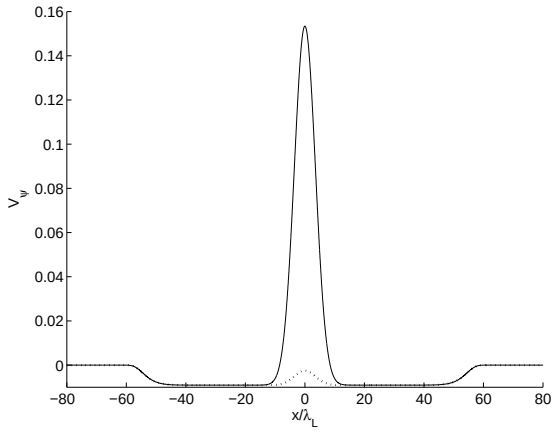

Figure 6. Initial potential experienced by the atom wave function for two different initial peak densities: $n_0 = 5.81\ 10^{18} m^{-3}$ (same as run (a), $\tilde{\psi}_0 = 0.0185$, dotted line), $n_0 = 1.44\ 10^{20} m^{-3}$ ($\tilde{\psi}_0 = 0.092$, solid line). The initial peak laser intensity and all other parameters are the same as for run (a). Normalization as in the text.

considered negligibly small. In this case the effect of resonance absorption on the BEC density modulations is small but will define the life time of these structures. Even at very large detunings, resonance absorption could come into play due to photoassociation which can be an effective mechanism of excitation of the high-lying vibrational levels of an excited molecule created from two atoms during a collisional process [22]. However, photoassociation spectra are in general known to be quite narrow and, comparing the range of detunings we are considering here with experimental data for photoassociation spectra, see for instance [23], shows that it is possible to neglect photoassociation effects in the parameter range considered for our model.

For too high initial values of $\tilde{\psi}_0$ we have found a new regime and a qualitatively different stationary state with the creation of two symmetric, mutually localized structures, moving outwards, see figure8. This is the result of having initially a central repulsive push not counterbalanced by the action of the laser in spite of the enhancement due to the chirp effect. The formation, dynamics and characteristics of these jet–like structures will be discussed elsewhere. A further increase in ψ_0 yields a dominant broadening of the atom laser function and a monotonous decrease of the peak atom density.

Increasing the initial laser peak intensity for a fixed initial atom density, also makes it possible to generate a continuous family of mutually localized solutions, see figure7(B) with examples of final stationary structures shown in figure9.

However, this also opens up the possibility of a collapse–like instability when the initial laser intensity is larger than a critical value which depends on the initial atom density. We have identified as collapsing cases, within the approximations of this model, those cases in which the peak atom density showed an increase towards the critical value corresponding to $\tilde{\psi}_0^2 = 1$, i.e. $n_* = 1.7\ 10^{22} m^{-3}$. From the numerical point of view, the propagation step required to maintain the error within given limits, decreases to zero. There seems to be a threshold intensity such that, above this, the

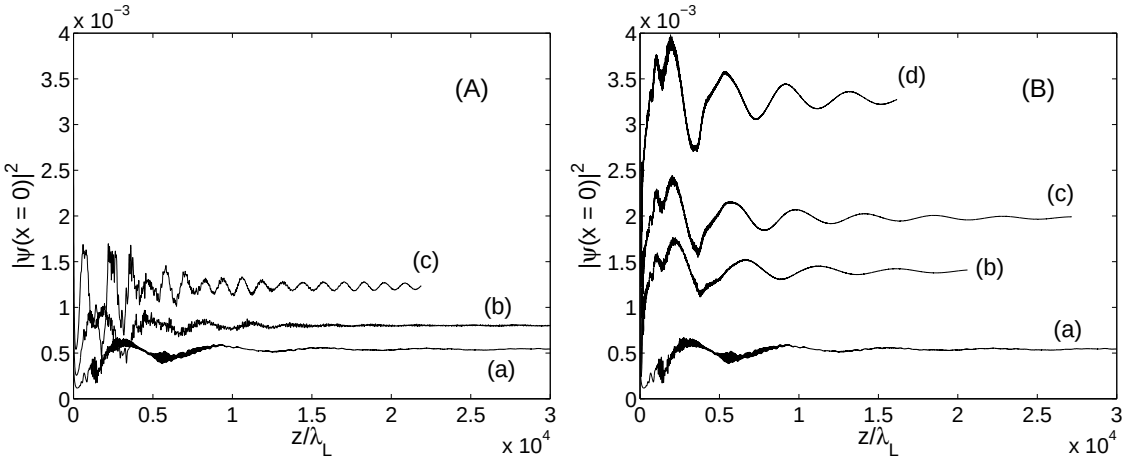

Figure 7. (A) Atom peak densities during propagation for fixed laser peak intensity $\tilde{a}_0 = 0.1346, I_0 = 0.0153mW/cm^2$ and (a) $\tilde{\psi}_0 = 0.0185, n_0 = 5.81\ 10^{18}m^{-3}$, (b) $\tilde{\psi}_0 = 0.0316, n_0 = 1.7\ 10^{19}m^{-3}$, (c) $\tilde{\psi}_0 = 0.054, n_0 = 4.96\ 10^{19}m^{-3}$. (B) Atom peak densities during propagation for fixed atom peak density $\tilde{\psi}_0 = 0.0185, n_0 = 5.81\ 10^{18}m^{-3}$ and (a) $\tilde{a}_0 = 0.1346, I_0 = 0.0153mW/cm^2$, (b) $\tilde{a}_0 = 0.3873, I_0 = 0.127mW/cm^2$, (c) $\tilde{a}_0 = 0.5477, I_0 = 0.254mW/cm^2$, (d) $\tilde{a}_0 = 1, I_0 = 0.847mW/cm^2$. Normalization as in the text.

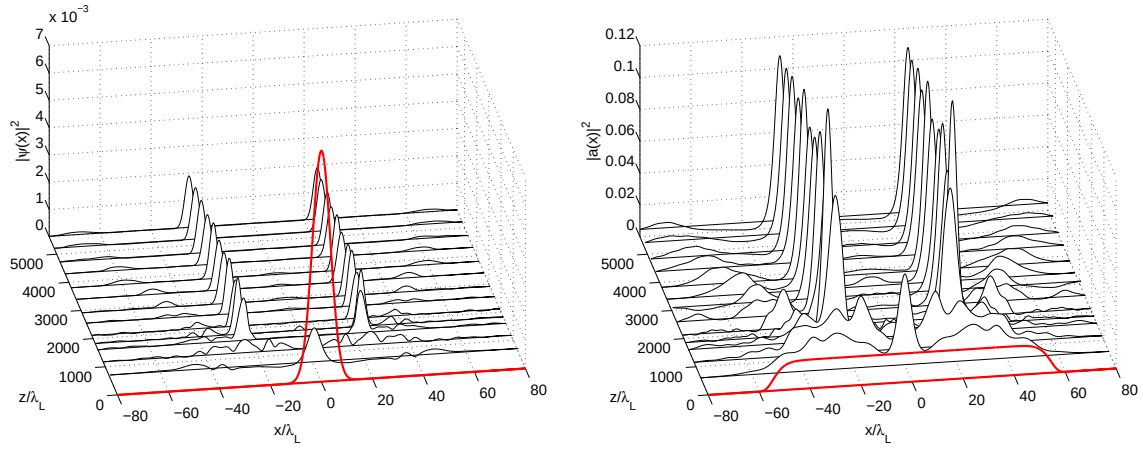

Figure 8. Structures formed starting from initial peak density $n_0 = 1.44\ 10^{20}m^{-3}$ (corresponding to the solid line potential in figure6). All other parameters are the same as for run (a). Normalization as in the text.

diffractive contributions to the atom dynamics can no longer balance the focusing effect of the dipole–dipole interaction anymore. Furthermore, due to the singular character of the focusing non linearity, this threshold decreases for higher initial atom densities. The numerically observed threshold intensities for collapse are given in figure10(A) for a range of initial atom densities. It is plausible that for low atom densities no collapse occurs, irrespective of how large the laser intensity is, however the corresponding extremely rapid dynamical features observed cannot be described under the hypothesis of the slowly varying envelope approximation. The effect of lowering the laser intensity

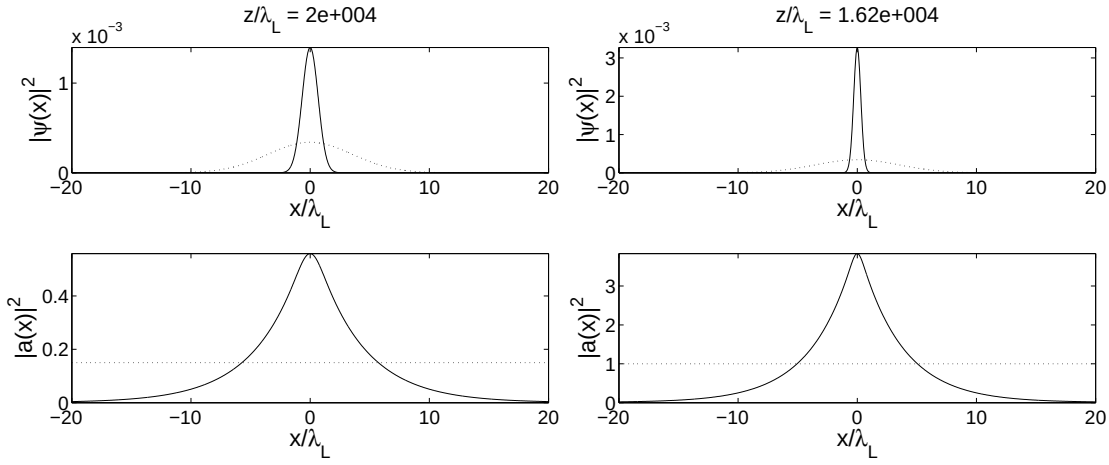

Figure 9. Left column: Stationary atom density and laser intensity after 1.99 $10^4\lambda_L$ of propagation along z for run(b) of figure7(B). Right column: after 1.61 $10^4\lambda_L$ of propagation along z for run(d) of figure7(B). Dotted lines: initial distributions. Normalization as in the text.

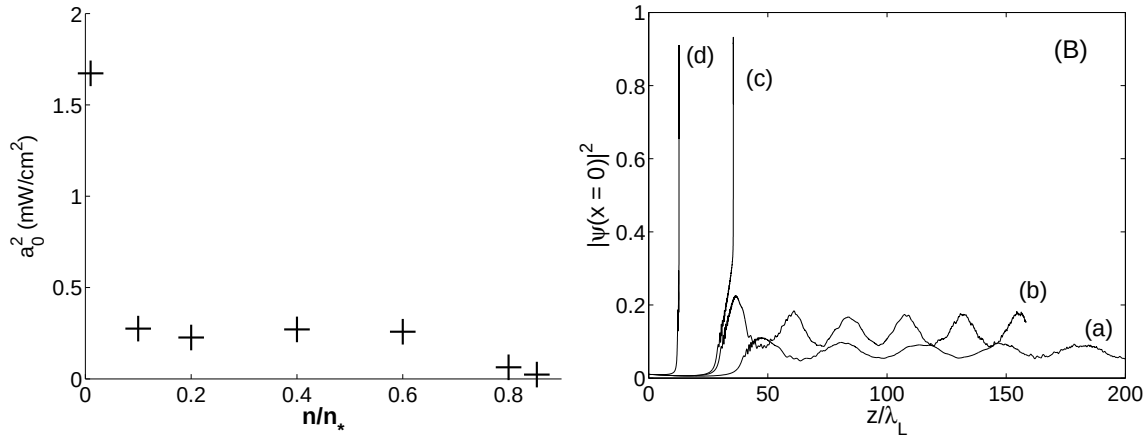

Figure 10. (A) Minimum initial laser intensity at which collapse was numerically observed for different values of the initial atom density n_0 given with respect to the critical one n_*. (B) Peak atom densities during propagation for varying initial laser intensities. For all cases $\tilde{\psi}_0 = 0.1, n_0 = 1.7\ 10^{20} m^{-3}$ and (a) $\tilde{a}_0 = 1, I_0 = 0.847 mW/cm^2$, (b) $\tilde{a}_0 = 1.8, I_0 = 1.52 mW/cm^2$, (c) $\tilde{a}_0 = 1.975, I_0 = 1.67 mW/cm^2$, (d) $\tilde{a}_0 = 10, I_0 = 8.47 mW/cm^2$. Normalization as in the text.

is shown in figure10(B) for a particular value of the initial atom density.

5. Conclusion

The present analysis has demonstrated that it should be possible to exploit the interaction of coherent electromagnetic radiation and BEC atomic beams to generate mutually localized structures. Assuming an initial flat–top profile for the laser intensity, the final peak densities and intensities as well as the widths of the generated structures,

depend on the initial conditions. It also seems possible to induce a collapse–like phenomenon on these systems. However, in such cases the model used here is insufficient and must be generalized to incorporate additional effects that are neglected in the present analysis.

Acknowledgments

F.C. would like to acknowledge the hospitality offered by the department of Radio and Space Physics of Chalmers University of Technology during the preparation of this work.

References

[1] Dalfovo F, Giorgini S, Pitaevskii LP, Stringari S 1999 *Rev. Mod. Phys.* **71** 463–512
[2] Cohen-Tannoudji C, Dupont-Roc J and Grynberg G 1998 *Atom-Photon Interactions* (Berlin: Wiley,).
[3] Craig D P and Thirunamachandran T 1984 *Molecular Quantum Electrodynamics* (London: Academic Press)
[4] Askhar'yan G A 1962 *Zh. Eksp. Teor. Fiz.* **42** 1567 [1962 *Sov. Phys JETP* **15** 1088]
[5] Ashkim A 1970 *Phys. Rev. Lett.* **25** 1321.
[6] Klimontovich Yu L and Luzgin S N 1979 *JETP Lett.* **30** 610.
[7] Saffman M 1998 *Phys. Rev. Lett.* **81** 65.
[8] Wallis H 1997 *Phys. Rev.* A **56** 2060.
Krutitsky K V, Burgbacher F and Audretsch J 1999 *Phys. Rev.* A **59** 1517.
[9] Giovanazzi S, O'Dell D and Kurizki G 2002 *Phys. Rev. Lett.* **88** 130402.
O'Dell D, Giovanazzi S, Kurizki G and Akulin V M 2000 *Phys. Rev. Lett.* **84** 5687.
[10] Avetisyan Yu A and Trifonov E D 2008 *JETP* **106** 426.
Kurizki G, Mazets I E, O'dell D and Schleich W P 2004 *IJMPB* **18** 961.
[11] Cattani F, Anderson D, Kim A and Lisak M 2005, *JETP Lett.* **81** 561.
[12] von Helmholtz 1881 *Wied. Ann.* **13** 385.
[13] Landau L D and Lifshitz E M 1960*Electrodynamics of Continuous Media* (New York: Pergamon Press).
[14] Pitaevskii L P 1961 *Sov. Phys. JETP* **39** 1008.
[15] Born M and Wolf E 1959 *Principles of Optics* (London: Pergamon Press)
[16] Balykin V I, Minogin V G and Letokhov V S 2000 *Rep. Progr. Phys.* **63** 1429.
[17] Dalfovo F, Giorgini S, Piatevskii L P and Stringari S 1999 *Rev. Mod. Phys.* **71** 463–512.
Leggett A J 2001 *Rev. Mod. Phys.* **73** 307–356.
[18] Cattani F, Geyko V, Kim A, Anderson D and Lisak M, submitted to *Phys. Rev.* A.
[19] Marcuse D 1981 *Appl. Opt.* **20** 3573.
Iwashita K, Nakagawa K, Nakano Y and Suzuki Y 1982 *Electron. Lett.* **18** 873.
[20] Agrawal G P 1995 *Nonlinear fiber optics* (London: Academic Press Limited).
[21] Parent A, Morin M and Lavigne P 1992 *Opt. Quantum Electron.* **24** 1071; Bagini V *et al.* 1996 *JOSA* A **13** 1385.
[22] Weiner J, Bagnato V S, Zilio S and Julienne P S 1999 *Rev. Mod. Phys.* **71** 1.
[23] Fioretti A, Amiot C, Dion C M, Dulieu O, Mazzoni M, Smirne G and Gabbanini C 2001 *Eur. Phys. J. D* **15** 189–198.

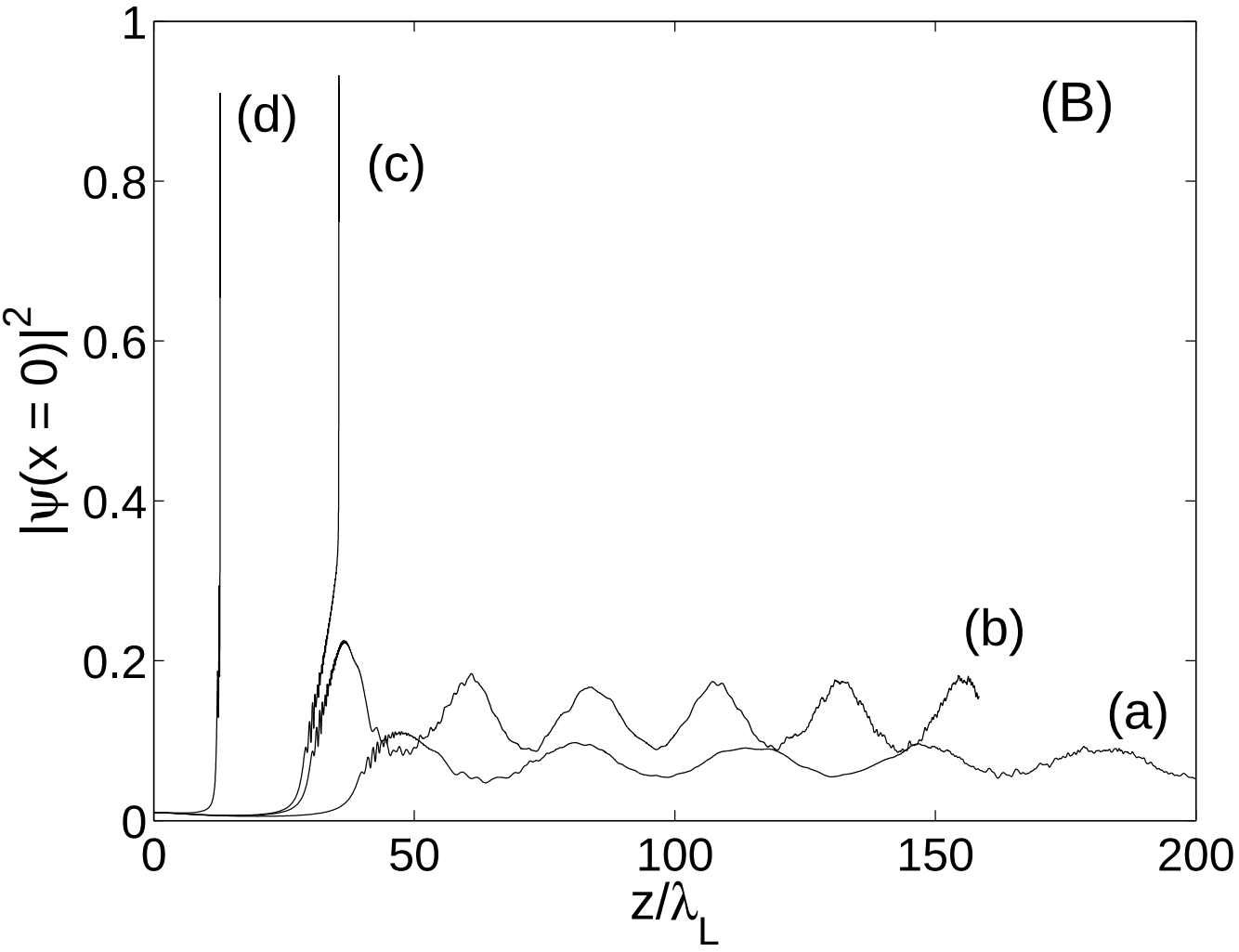

Figure 10 b (figure15.eps)